

Supplement of Biogeosciences, 16, 1583–1605, 2019  
<https://doi.org/10.5194/bg-16-1583-2019-supplement>  
© Author(s) 2019. This work is distributed under  
the Creative Commons Attribution 4.0 License.



*Supplement of*

## **Patterns of suspended particulate matter across the continental margin in the Canadian Beaufort Sea during summer**

**Jens K. Ehn et al.**

*Correspondence to:* Jens K. Ehn ([jens.ehn@umanitoba.ca](mailto:jens.ehn@umanitoba.ca))

The copyright of individual parts of the supplement might differ from the CC BY 4.0 License.

### *Seasonal development in the Canadian Beaufort Shelf during 2009*

The MALINA expedition was conducted from 31 July to 24 August 2009 in the southeastern Beaufort Sea onboard the research icebreaker *CCGS Amundsen* (Fig. 1). This supplementary section briefly describes the seasonal development of surface conditions, based on satellite imagery, leading up to the MALINA expedition.

The southeastern Beaufort Sea was fully ice covered from the end of November 2008 to mid-May 2009 when the flaw lead, called Cape Bathurst Polynya, began to open up along the mouth of Amundsen Gulf. By June 2009, the Cape Bathurst Polynya had formed into an open water strip between the landfast ice and the offshore pack ice, which extended the full length of the Canadian Beaufort Sea shelf. This is a feature that reoccurs each year but displays considerable temporal variability (Galley et al., 2008). The annual peak of river discharge ( $>25,000 \text{ m}^3 \text{ s}^{-1}$  measured at the Arctic Red River location; see Fig. 10a) in early June was extensively hindered from entering offshore waters by the solid landfast ice cover and its thick, deformed border, the Stamukhi zone. MODIS satellite images (Figures S1 and S2) show that ice break-up occurred progressively towards east in Amundsen Gulf during the first half of June and ice floes moved westward partly covering the shelf in response to sustained easterly winds. In fact, easterly along-shelf winds persisted throughout June (see Fig. 11a). The landfast ice along the river delta, however, remained fast. The MODIS satellite images also reveal a river plume that extended from the landfast ice edge in Mackenzie Bay (westernmost part of the shelf) northwest into the pack ice (Figure S2).

Mackenzie River water began overflowing the landfast ice cover by mid-June. The landfast ice cover gradually broke up during the latter part of June 2009 starting from Mackenzie Bay in the west and moving east. During this time, satellite imagery revealed large turbid surface plumes that extended northwest into the pack ice. In early July, only a section of possibly grounded landfast ice remained north of Beluga Bay and numerous ice floes were scattered over the shelf.

Wind direction changed to northwesterly in July, and wind speeds decreased markedly by the end of the month. Consequently, the river plume changed direction to flow east along the coast.

Satellite images of the period reveal a surface plume extending north of Cape Bathurst into Amundsen Gulf. Such eastward flow is a typical response of the river outflow in the absence of winds (e.g., Carmack and Macdonald, 2002). Weak winds also kept the broken-up landfast ice floes on the shelf and the Beaufort Sea pack ice margin extended further south compared to previous and following years.

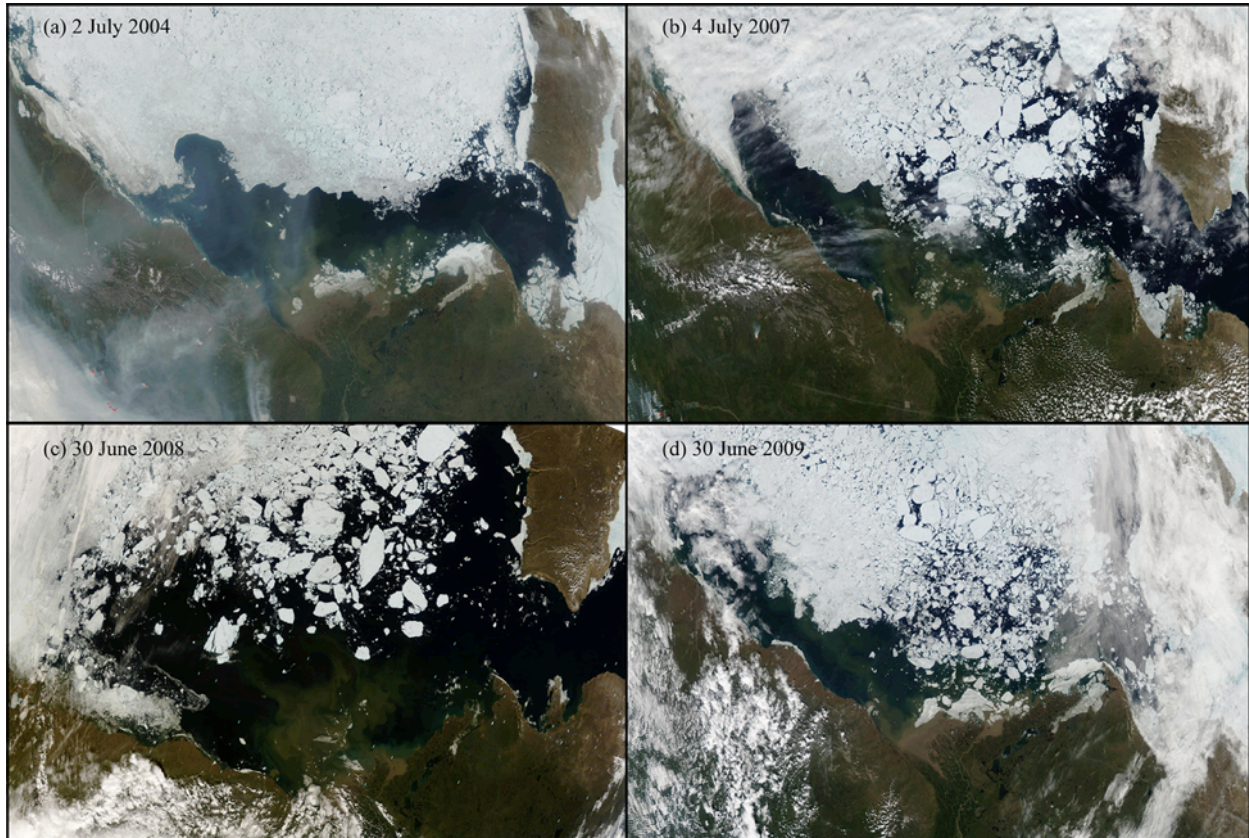


**Figure S1.** MODIS true-color images of the surface conditions in southern Beaufort Sea during the June to July cross-over during four years.

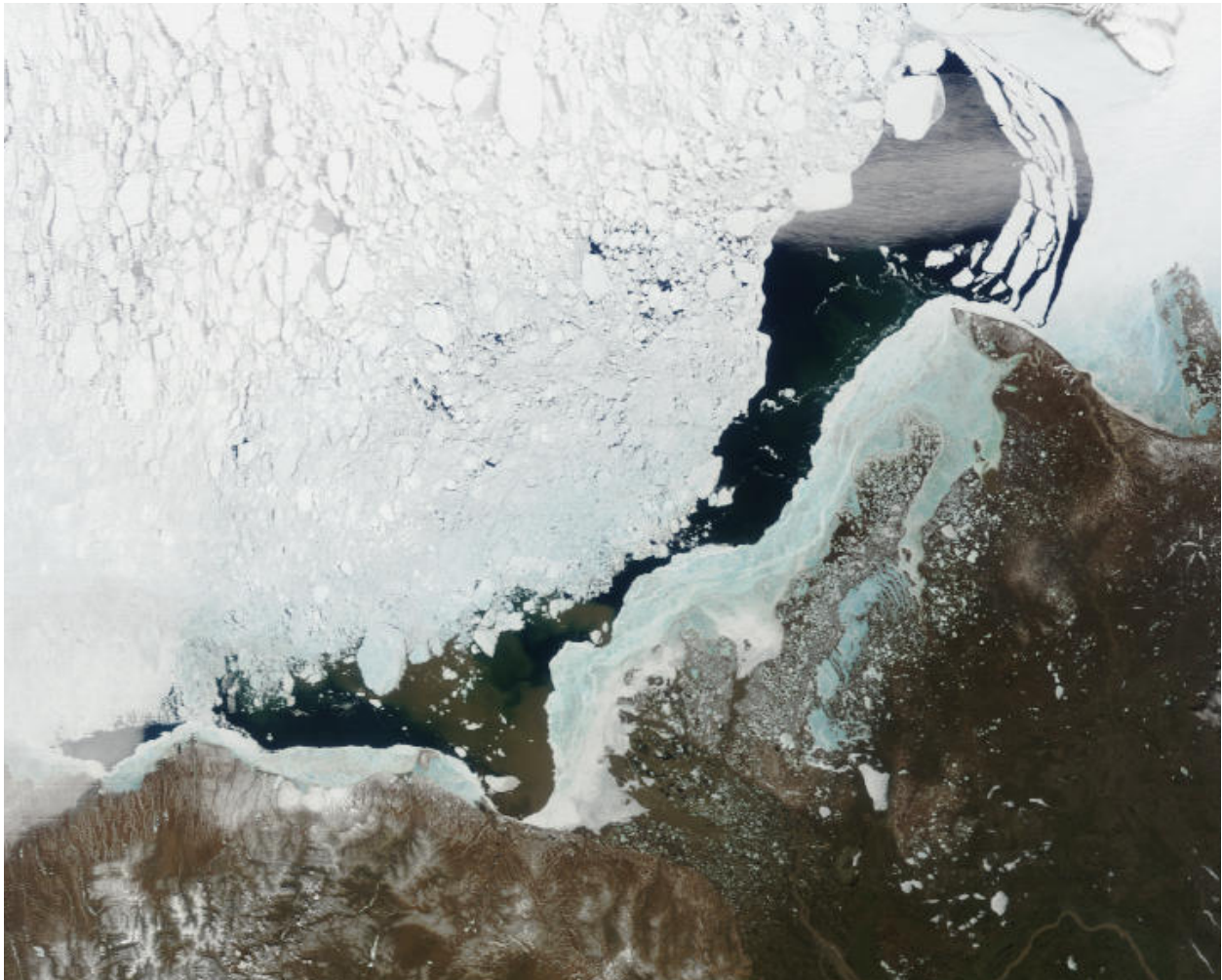


**Figure S2.** Cut out of study region from MODIS true-color image for yearday 156 (June 4) in 2009 (crefl1\_143.A2009156205000-2009156205500.1km.jpg). A sediment-laden plume is seen extending northwestward from the landfast ice edge to the pack ice.

#### *Examples of river plume inertia*

Figure S3 shows MODIS imagery of sea-surface temperature that highlights the effects of river plume inertia. Figure S3a shows how the invading plume reached northwest past the ice edge (located at about 71°N) creating a 130 km long and 80 km wide ice-free area and apparently affecting the surface temperature of the ice field for an additional 250 km. Thus, the plume may have extended more than 650 km from the river mouth and affected the sea ice cover over a distance of 380 km. At the same time of the 2009 season (Figure S3b), the plume did not appear to have an effect on ice surface temperatures (mainly thicker multi-year ice) past the ice edge located about 260 km from the river mouth.

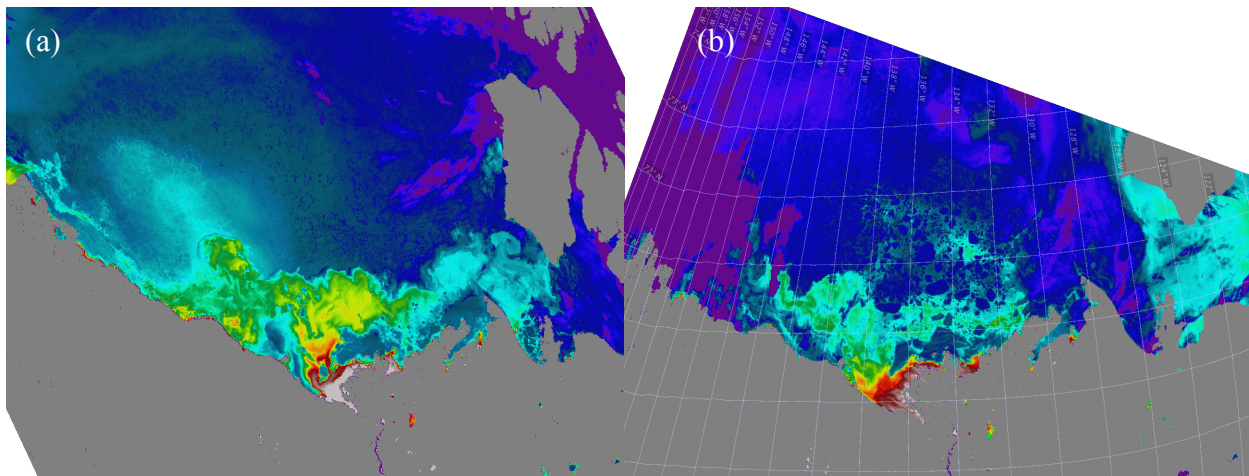


**Figure S3.** MODIS sea surface temperature scenes for the Beaufort Sea. Temperature scale is linear from  $-1^{\circ}\text{C}$  (purple) to  $14^{\circ}\text{C}$  (dark red). Scene (a) was taken on 2 July 2004, while the scene in (b) was taken on 30 June 2009.

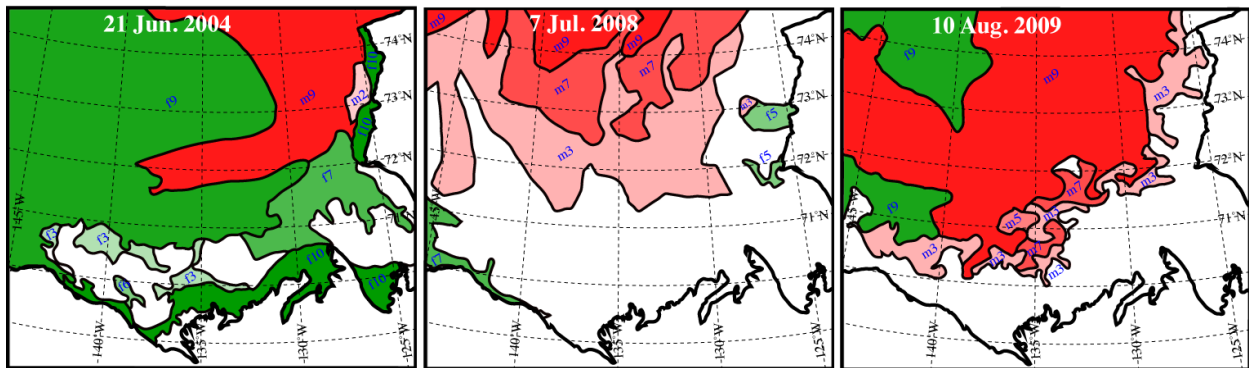


**Figure S4.** Ice coverage data from the Canadian Ice Service. The blue labels denote areas of first-year ice ('f') and multi-year ice ('m'), while numbers that follow indicate ice concentration in tenths (9+ indicates  $> 90\%$ ). The areas of the two ice types are also associated with colours, green for first-year ice, and red for multi-year ice. The shade of the colours relate to ice concentration.

#### *Regression analysis for SPM vs. $c_p(660)$ and POC vs $c_p(660)$*

Three types of regression analysis for SPM vs.  $c_p(660)$  and POC vs  $c_p(660)$  were evaluated: (i) a linear fit, (ii) a linear fit to log-transformed data, and (iii) a nonlinear power function fit using the Levenberg-Marquardt optimization algorithm (Fig. S5). For the SPM vs.  $c_p(660)$  the differences between the three types of regressions are not significant in terms of the determination coefficient ( $r^2$ ) which was 0.711 for the linear fit and 0.713 for the other fits. However, the nonlinear power function fit appears to match the SPM vs.  $c_p(660)$  data the best. This is supported by reasonably good values of both the root mean square error (RMSE =  $0.421 \text{ g m}^{-3}$ )

and mean normalized bias (MNB = 13.7%). MNB and RMSE were calculated following equations in Stramski et al. (2008):

$$\text{MNB} = \frac{1}{N} \sum_{i=1}^N \left( \frac{P_i - O_i}{O_i} \right) 100,$$

$$\text{RMSE} = \left[ \frac{1}{N-m} \sum_{i=1}^N (P_i - O_i)^2 \right]^{\frac{1}{2}},$$

where  $P_i$  is the variable predicted from the regression,  $O_i$  is the observed variable,  $N$  is the number of observations, and  $m$  is the number of coefficients in the regression fit (i.e.,  $m = 2$ ). For comparison, these values were: RMSE = 0.421 g m<sup>-3</sup> and MNB = 26.0% for linear fit, and RMSE = 0.457 g m<sup>-3</sup> and MNB = 11.1% for linear fit based on log-transformed data. Therefore, we selected the SPM vs.  $c_p(660)$  relationship obtained from the power function fit using nonlinear least squares regression to ordinary (non-transformed) variables as the algorithm for estimating SPM in [g m<sup>-3</sup>] from  $c_p(660)$  in [m<sup>-1</sup>] in the rest of this study:

$$\text{SPM} = 1.933 c_p(660)^{0.9364}. \quad (\text{Eq. 2})$$

The regression analysis of POC vs.  $c_p(660)$  data yielded the best results for linear fit to log-transformed data:  $r^2 = 0.744$ , RMSE = 0.0449 g m<sup>-3</sup>, and MNB = 8.72%. These statistics are, however, only slightly better compared with the other two regression analyses (linear fit: RMSE = 0.0459 g m<sup>-3</sup> and MNB = 36.16%, nonlinear power function fit: RMSE = 0.0436 g m<sup>-3</sup> and MNB = 22.7%). Hence, for POC we recommend the algorithm obtained from a linear regression to log-transformed data:

$$\text{POC} = 0.2071 c_p(660)^{0.6842}, \quad (\text{Eq. 3})$$

where POC is in [g m<sup>-3</sup>] and  $c_p(660)$  in [m<sup>-1</sup>].

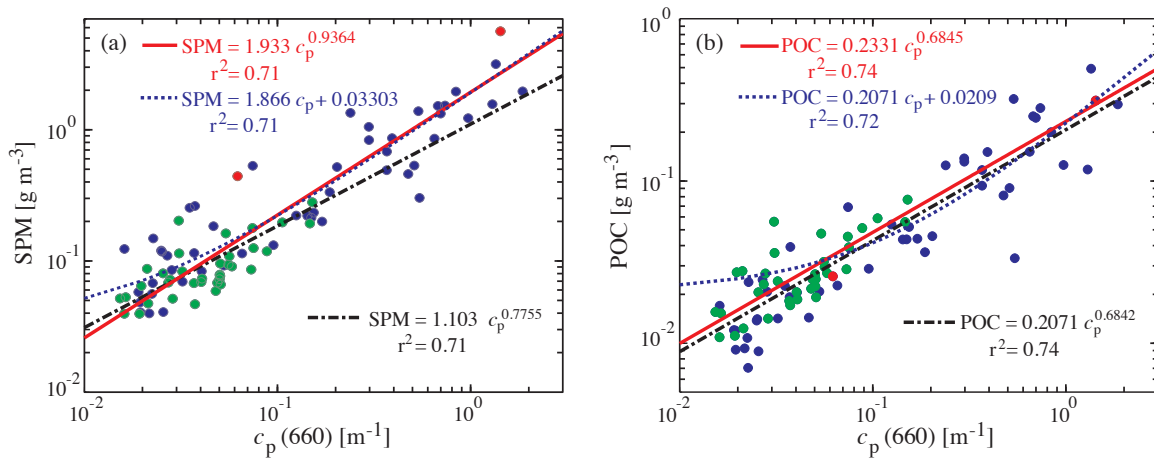


**Figure S5.** (a) SPM and (b) POC versus beam attenuation coefficient measured using the CTD/Rosette deployments on the Amundsen during MALINA 2009. The colors of the data points indicate POC/SPM categories: mineral-dominated (red), mixed (blue), and organic-dominated (green). Notwithstanding the colours, all data points are used for the regressions. The solid red lines are nonlinear power function fits, the blue dotted lines are linear fits, and the dash-dotted black lines are linear fits to log-transformed SPM or POC data. The regression equations and determination coefficient ( $r^2$ ) are displayed in the graphs.

**Table S1.** List of station locations and sampling times during MALINA 2009

Station	Latitude	Longitude	Date	Time (UTC)	Bottom depth (m)
390	70.180465	-133.56225	7/31/09	21:03	58
690	69.487517	-137.94252	8/01/09	12:22	54
680	69.607452	-138.20672	8/02/09	16:45	122
394	69.847252	-133.49265	8/03/09	20:28	14
290	70.672792	-130.43468	8/04/09	12:15	33
280	70.869285	-130.50783	8/04/09	14:53	42
270	71.07381	-130.5482	8/04/09	19:50	56
260	71.266588	-130.60843	8/04/09	22:01	58
250	71.472513	-130.6972	8/06/09	04:20	219
240	71.672713	-130.74145	8/05/09	06:15	462
230	71.866097	-130.83832	8/05/09	08:00	704
220	72.058367	-130.8924	8/05/09	10:10	899
240	71.671288	-130.72675	8/05/09	22:07	459
110	71.701008	-126.48272	8/06/09	11:04	401
120	71.564288	-126.90622	8/06/09	22:51	419
130	71.426768	-127.36102	8/08/09	00:46	311
140	71.284297	-127.79155	8/07/09	09:00	151
150	71.15902	-128.16008	8/07/09	11:11	66
160	71.049063	-128.49655	8/07/09	12:35	43
170	70.911813	-128.92155	8/07/09	14:35	35
150	71.161882	-128.15295	8/07/09	22:52	66
390	70.177278	-133.56082	8/08/09	11:31	47
380	70.396942	-133.6074	8/08/09	13:07	63
370	70.5983	-133.65238	8/08/09	19:03	75
360	70.800825	-133.73687	8/08/09	21:51	78
350	70.97161	-133.73318	8/10/09	04:18	91
340	71.173652	-133.83982	8/09/09	06:16	575
330	71.37328	-133.90055	8/09/09	08:00	1086
320	71.57073	-133.94048	8/09/09	10:07	1156
310	71.743327	-133.9468	8/09/09	12:31	1614
320	71.570683	-133.958	8/09/09	15:00	1159
330	71.369112	-133.88802	8/09/09	21:25	1082
340	71.17138	-133.82583	8/09/09	23:44	578
680	69.60422	-138.22625	8/10/09	16:40	125
670	69.797617	-138.44068	8/10/09	19:16	174
660	69.982892	-138.64177	8/12/09	00:52	268
650	70.165613	-138.91048	8/12/09	05:32	375
640	70.3397	-139.1497	8/11/09	07:30	564
630	70.535787	-139.38122	8/11/09	09:06	839
620	70.703868	-139.60865	8/11/09	11:04	1708
610	70.792795	-139.60125	8/11/09	14:23	1823
620	70.679543	-139.62673	8/11/09	18:38	1590



630	70.533458	-139.37952	8/13/09	00:47	838
640	70.33845	-139.13603	8/13/09	02:45	573
760	70.554242	-140.79845	8/12/09	13:44	578
770	70.347943	-140.81422	8/12/09	22:57	223
780	70.156278	-140.80747	8/14/09	01:53	49
695	69.2064	-137.0065	8/13/09	16:11	5
694	69.2465	-137.1866	8/13/09	17:48	8
697	69.1298	-136.6816	8/13/09	20:29	2
696	69.16	-136.8064	8/13/09	21:34	3
691	69.3833	-137.7788	8/14/09	00:19	43
693	69.2963	-137.3891	8/14/09	01:41	30
345	71.330417	-132.56597	8/14/09	16:22	479
570	70.222535	-137.25873	8/17/09	10:38	55
560	70.389308	-137.47027	8/17/09	12:07	400
550	70.57146	-137.70617	8/17/09	14:04	1076
540	70.751188	-137.8917	8/17/09	17:15	1514
398	69.5142	-133.4125	8/16/09	18:10	3
397	69.5948	-133.4339	8/16/09	19:56	5
396	69.679416	-133.456	8/16/09	20:55	6
395	69.7594	-133.4582	8/16/09	22:15	9
393	69.9289	-133.5057	8/15/09	n/a	17
392	70.0118	-133.522	8/15/09	n/a	27
391	70.0946	-133.5389	8/15/09	n/a	35
530	70.941595	-138.15322	8/19/09	04:28	1602
430	71.21747	-136.72022	8/18/09	14:57	1351
440	71.033162	-136.46573	8/20/09	00:05	1149
450	70.854652	-136.23135	8/20/09	02:25	840
470	70.47029	-135.90993	8/19/09	06:00	70
480	70.274523	-135.75897	8/19/09	07:25	60
460	70.677875	-136.04735	8/19/09	13:40	468
135	71.31142	-127.46623	8/20/09	18:36	228
235	71.76446	-130.83017	8/22/09	08:30	619
235	71.761465	-130.76027	8/22/09	10:37	568

---